Anatomical Markov Prior-based Multimodality Image Registration

Kathleen Vunckx[1,2], Frederik Maes[2,3], Johan Nuyts[1,2]

***Abstract*—Some similarity measures used in state-of-the-art multimodality image registration algorithms, (e.g., mutual information (MI)) have been shown to be suitable anatomical priors for maximum a posteriori reconstruction in emission tomography. Therefore, it is reasonable to assume that some originally designed anatomical priors may also be well suited for multimodality image registration. In this work, we evaluate the registration performance of three variants of an anatomical Markov prior, previously proposed by Bowsher et al. First, simulated data are used to verify whether the suggested registration criteria yield an optimum when an FDG positron emission tomography (PET) image and a T1-weighted magnetic resonance (MR) image of a human brain are perfectly aligned. Next, the registration accuracy of the proposed criteria is assessed for PET to MR and MR to PET registration of simulated human brain images, and compared to the accuracy reached by MI. Last, the new methods are applied to challenging measured rat and mouse brain data sets, consisting of low resolution FDG microPET images and high resolution microMR images with a strong bias field. It was shown that the anatomy-based Markov priors indeed yield a well-defined optimum for aligned PET-MR images and that similar registration accuracy can be achieved as with MI, especially for registration to MR images suffering from a bias field. Nevertheless, in contrast to MI, the new criteria usually require a good initial guess of the transformation parameters in order not to get stuck in a local optimum. The proposed methods are shown to be superior to MI for registering measured microMR brain images with a strong bias field to FDG microPET images if a good initialization is provided.**

I. Introduction

The multimodality image registration field is currently dominated by algorithms exploiting information theory measures, such as mutual information (MI) [1] and normalized mutual information (NMI) [2]. These measures recently also found their way to the image reconstruction domain. MI [3] and joint entropy (JE) [4] have been used to extract joint information in an emission and an anatomical image, serving as an anatomical prior in maximum a posteriori reconstruction to improve the resolution and quantitative accuracy of the emission image. Since successful registration algorithms have been shown to be appropriate as anatomical priors, promising anatomical priors might also be good for multimodality image registration.

In this work, we study the registration performance of a Markov prior, proposed by Bowsher *et al.* as an anatomical prior [5]. The rationale behind this anatomical prior is as follows: typically the activity distribution in emission tomography images is (at least locally) well correlated with the anatomical information. Therefore, it is beneficial to encourage neighboring voxels that are similar in the anatomical image to have similar values in the emission image by applying a Markov prior to these voxels during reconstruction. For the same reason, it is to be expected that a similarity measure for this selection of Markov cliques will reach an optimum when the two images are perfectly registered. In this paper, this hypothesis is evaluated and endorsed by studies using simulated as well as real PET and MR images.

[1] Dept. of Nuclear Medicine, K.U. Leuven, B-3000 Leuven, Belgium.
[2] Medical Imaging Research Center, K.U. Leuven, B-3000 Leuven, Belgium.
[3] Center for Processing Speech and Images, Department of Electrical Engineering, K.U. Leuven, B-3000 Leuven, Belgium.

This work is supported by the Research Foundation - Flanders, by the SBO grant 060819 "Quantiviam" of IWT, by IAP-grant P6/38 of the Belgian Science Policy, and by the IMIR project of the K.U. Leuven.

II. Theory

The registration algorithms proposed in this manuscript are based on an anatomical prior, described by Bowsher et al. in [5], and further explored by several other groups for enhancing emission tomography reconstruction [6]–[8]. Therefore, we first briefly explain how information from an anatomical and a functional image can be combined using a Markov log-prior (MP) function (Section II-A). In section II-B, a criterion for multimodality image registration is derived from this MP function. Finally, the selection of similarity measures evaluated in this paper is presented (Section II-C).

A. Anatomical Markov prior

The anatomical prior proposed by Bowsher et al. [5] can be considered as a standard Markov prior with an anatomy-based neighbor selection. The general expression for this Markov log-prior typically used in a penalized likelihood algorithm is

$$M(\Lambda) = \sum_j \sum_k w_{jk} S(\lambda_j, \lambda_k), \text{ with } w_{jk} \neq 0 \text{ if } \; k \in N_j \tag{1}$$

with Λ the emission image, j and k the voxel indices, w_{jk} a neighbor-dependent weight, N_j the Markov (i.e. local) neighborhood of voxel j, and $S(\lambda_j, \lambda_k)$ a measure for the similarity between the estimated activity in voxels j and k.

Unlike for the traditional Markov priors, an anatomy-dependent neighbor selection is performed in the 'Bowsher' Markov prior. For each voxel j, the local neighborhood N_j is scanned in the anatomical image and only the B neighbors that are most similar to j (i.e. least absolute difference in intensity) are assigned a non-zero weight. In this work, we restrict the weights to either 1 or 0, although it could easily be extended to distance-based or similarity-based weights.

B. Registration algorithm

For multimodality image registration, the following criterion C is proposed, which needs to be minimized:

$$\begin{aligned} C &= \frac{-M(\tilde{F},\tilde{R})}{N_O} \\ &= -\frac{\sum_j \sum_k w_{jk}(\tilde{R}) S(\tilde{f}_j,\tilde{f}_k)}{N_O} \\ \text{with} \quad & w_{jk}(\tilde{R}) = 1, \text{ if } k \in N_j(\tilde{R}) \\ & w_{jk}(\tilde{R}) = 0, \text{ otherwise.} \end{aligned} \tag{2}$$

$\tilde{F}$ is the transformed floating image with intensities $\tilde{f}_j$ and $\tilde{f}_k$ in voxels j and k, respectively, that is to be registered to reference image R. $\tilde{R}$ equals R except for voxels with intensities in $\tilde{F}$ or R below a chosen background level set to zero to exclude the background during registration. The criterion is normalized w.r.t. the region of overlap of $\tilde{F}$ and $\tilde{R}$ by dividing by N_O, the number of included voxels. $N_j(\tilde{R})$ is the set of neighboring voxels of voxel j that was selected based on the similarity in the reference image.

C. Similarity measures

To quantify the similarity between selected neighboring voxels in $\tilde{F}$, a quadratic (QU), absolute value (AV) [9] and relative difference (RD) figure of merit was deduced from Markov log-prior functions commonly used in emission tomography reconstruction [9], [10]:

$$S_{QU} = -\frac{(\tilde{f}_j - \tilde{f}_k)^2}{2\delta}, \text{ with } \delta = 1 \tag{3}$$

$$S_{AV} = -|\tilde{f}_j - \tilde{f}_k| \tag{4}$$

$$S_{RD} = -\frac{(\tilde{f}_j - \tilde{f}_k)^2}{\tilde{f}_j + \tilde{f}_k + \gamma|\tilde{f}_j - \tilde{f}_k|}, \text{ with } \gamma = 0 \tag{5}$$

III. Simulation studies

In this section, first an experiment is described for verification of the hypothesis that the proposed criteria reach a minimum when two images are aligned. Next, we elaborate on the validation of the registration algorithms using PET and MR simulated data. As they are by definition perfectly registered, the accuracy of the registration can be compared to that of state-of-the-art algorithms.

For all registrations, trilinear interpolation was used to resample the images, except if mentioned otherwise. Furthermore, all MP registrations were initially performed at 4 times lower resolution, going over twofold downsampling to full resolution to increase the stability. To calculate the Markov-based registration criterion C, the 10 most similar voxels in the reference image were selected in a local, spherical 5×5×5 neighborhood of each voxel. This can be performed beforehand and stored, reducing the calculation time during image registration.

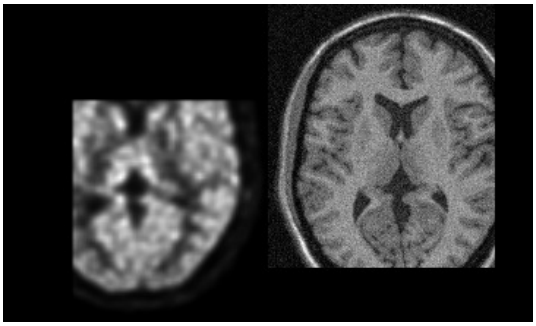

Fig. 2. Truncated PET and MR image used in the proof of concept study. All images were sampled with 1 mm×1 mm×1 mm voxels.

A. Proof of concept

To verify whether the suggested algorithms indeed yield a minimum value for C when an emission and an anatomical image are aligned, the three MP criteria (eq. (3)-(5)) were evaluated for a simulated noisy MR image and an FDG PET image (post-smoothed maximum likelihood expectation maximization (MLEM) reconstruction) rotated around and translated along the three main axes (see Fig. 1). Because the simulated PET data were derived from the simulated MR (T1-weighted image from the Brainweb database [11], [12]), the initial PET image was perfectly aligned to the MR image. During transformation, the PET (2.25 mm×2.25 mm×2.425 mm) was resampled to the MR voxel size (1 mm×1 mm×1 mm). Rotations ([-45°, 45°], step: 1°) and translations ([-45 mm, 45 mm], step: 1 mm) were applied in three orthogonal directions.

The same study was repeated for truncated versions of the PET and MR image (see Fig. 2) to reject the hypothesis that a minimum is reached because the number of overlapping voxels is maximized.

B. Validation Study

To assess the accuracy of the new registration methods, the same post-smoothed FDG PET reconstruction as above was used in combination with three perfectly registered, simulated T1-weighted MR images from the Brainweb database [11], [12]: a noise-free MR, a noisy MR, and a noisy MR with bias field (see Fig. 1). The three MR images were first rigidly transformed to 10 random locations (max. rotation: 5°, max. translation: 10 mm). Next, the PET image was registered to these 3×10 images using the three MP registration algorithms. By interchanging the role of the floating and the reference image in this study, the accuracy of MR to PET registration was also evaluated. The registration accuracy was quantified by computing the mean and maximum absolute distance between 8 reference points located at the vertices of the volume enclosing the brain. For comparison, the accuracy obtained with MI using trilinear (TRI) and partial volume (PV) interpolation was calculated too (using MIRIT [1]).

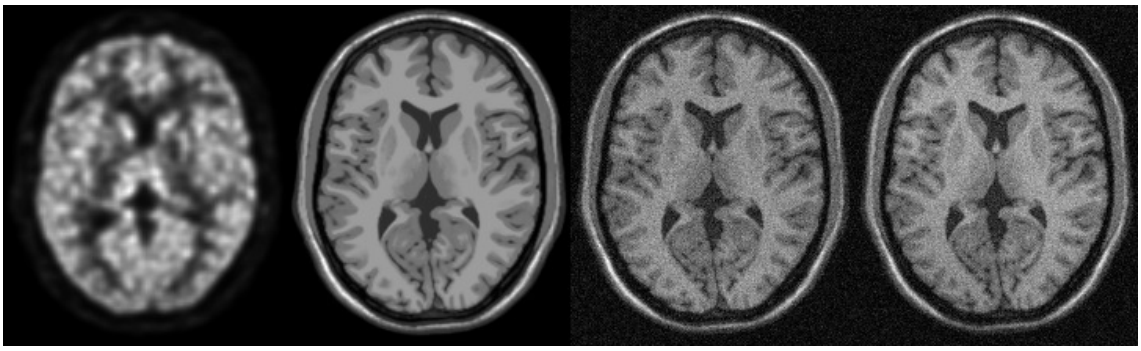

Fig. 1. (Left to right: transaxial slices through the PET, the noise-free MR image, the noisy MR image, and the noisy MR image with bias field. For visualization purposes, all images were sampled with 1 mm$\times$1 mm$\times$1 mm voxels.

IV. Evaluation on Measured Data

A. Rat Brain Data

The robustness of the proposed methods was evaluated on a subset of an existing rat brain data set [13]. Five wild type rats and five rats of a transgenic Huntington's disease model were selected randomly. All animals have been scanned for 40 minutes on a Focus 220 microPET system (Siemens/Concorde Microsystems, Knoxville, TN) 60 minutes after [^{18}F]-FDG injection. The images were reconstructed using the MLEM algorithm and post-smoothed with a Gaussian kernel with a full-width at half-maximum of 1.1 mm. All animals have also received a high resolution microMR scan on a 9.4 Tesla Bruker Biospec Scanner (Bruker Biospin, Ettlingen, Germany) using a dedicated rat brain surface coil (Rapid Biomedical, Rimpar, Germany) and applying a 3D turboRARE sequence.

In this study, MR to PET registration was performed on the non-processed images using the MP algorithms as well as MI and normalized MI (NMI) [2] for comparison. A proper initialization of the transformation parameters was obtained by a rough manual registration. For all registration algorithms the same initialization was used.

B. Mouse Brain Data

To show that the use of the MP criteria for registration is not limited to data sets with a high level of detail in the MR image, the same methods were applied to a mouse data set (FDG microPET and noisy microMR using a 3D turboRARE sequence). Because of the small dimensions of a mouse brain, relatively less anatomical information is available in this MR image. In addition, the MR image suffers from more severe bias field artifacts and noise compared to the MR images of the rat brains.

V. Results

A. Proof of concept

Fig. 3(a)-(c) show that all three methods yield a well-defined local minimum in perfectly registered position (rotation/translation equal to zero). In addition, this test gives an indication that the methods will not easily get trapped in a local optimum, except when translating in the plane-direction (i.e. along the axis of rotation). When applying the MP criteria to the truncated images, still a clear local minimum is identified at the position where the images are perfectly aligned (see Fig. 4). However, registration of these images will require a better initialization of the transformation parameters.

TABLE II
Accuracy of the rat brain registrations.

method	very good	good	bad
MP QU	6	4	0
MP AV	8	2	0
MP RD	8	2	0
MI TRI	1	6	3
MI PV	1	6	3
NMI TRI	1	6	3
NMI PV	1	6	3

B. Validation study

The results of the human brain image registration studies are listed in Table I. In the first column, the evaluated registration method is mentioned. In the second column, the accuracy of the PET to MR registrations is presented. In the last column, the accuracy of the MR to PET registrations is shown. In each first subcolumn, the number of successful registrations (out of 10) is given. In the following three subcolumns, the mean (maximum) absolute distance in the column, row and plane direction is presented, respectively.

All PET to MR and MR to PET registrations were successful, i.e. the maximum distance between the reference points in PET and MR was below 3 mm in all directions. MI achieved very good accuracy for all images. Partial volume interpolation was typically slightly better than trilinear interpolation, especially for the MR to PET registrations.

The MP criteria reached about the same accuracy level as MI with trilinear interpolation. The largest difference was observed in the accuracy in the plane direction (along the axis of rotation), where MI PV outperformed the MP methods in particular when no bias field was present in the MR image.

C. Rat Brain Data

Because no ground truth was available for the microMR to microPET registration, evaluation was performed by an expert in pre-clinical image analysis, based on visual comparison of

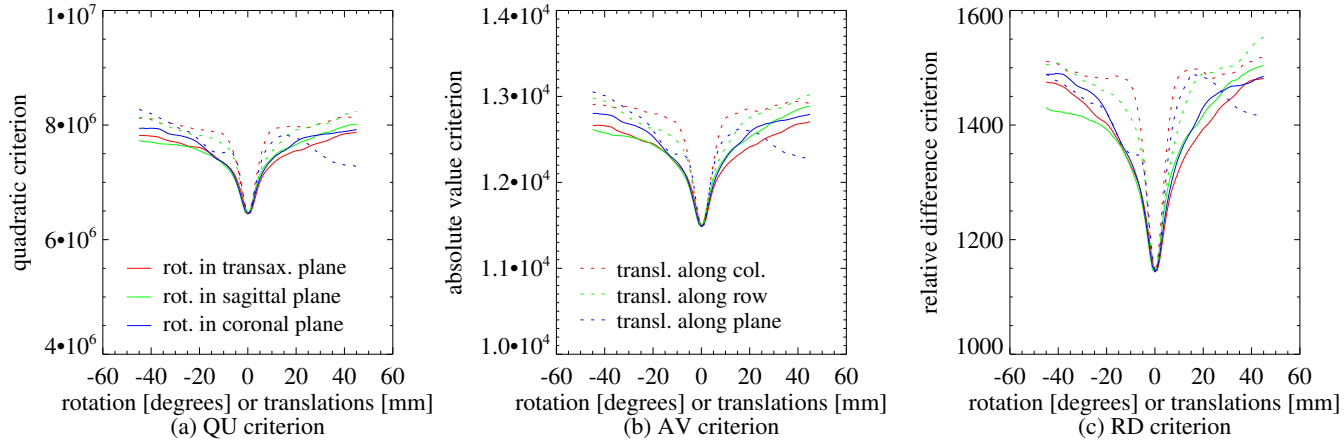

Fig. 3. Proof of concept study: simulated human brain PET and MR images. Plots of the (a) quadratic, (b) absolute value and (c) relative difference cost function vs. the rotation (solid lines) and translation offset (dotted lines).

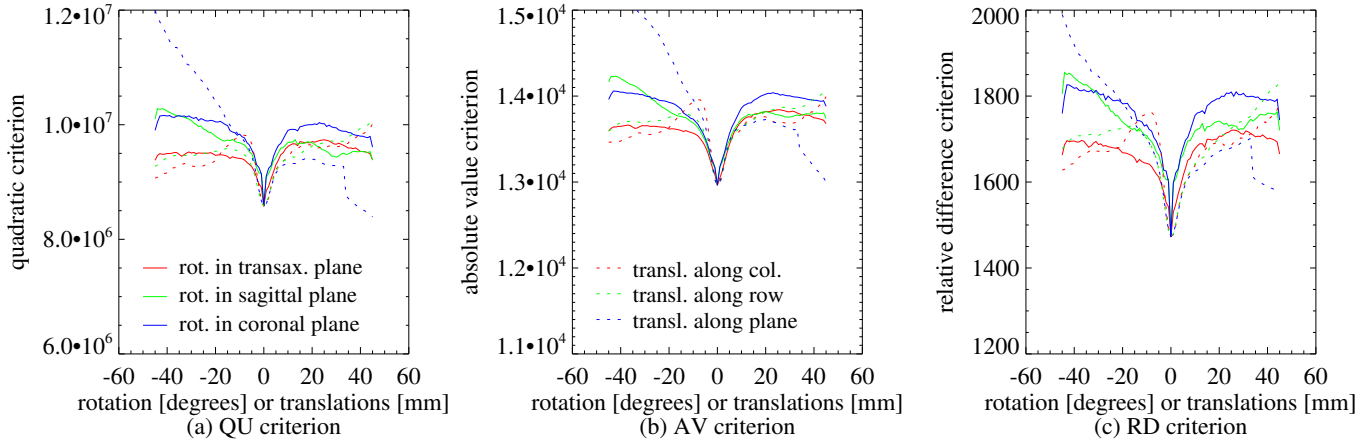

Fig. 4. Proof of concept study: truncated simulated human brain PET and MR images. Plots of the (a) quadratic, (b) absolute value and (c) relative difference cost function vs. the rotation (solid lines) and translation offset (dotted lines).

TABLE I
REGISTRATION PERFORMANCE EXPRESSED AS NUMBER OF SUCCESSES AND MEAN (MAXIMUM) ABSOLUTE DISTANCE IN MM BETWEEN THE REFERENCE POINTS IN THE MR AND THE PET IMAGE.

	no.	column	row	plane	no.	column	row	plane
method	PET -> noise-free MR				noise-free MR -> PET			
MP QU	10	0.78 (1.40)	0.66 (1.28)	0.30 (0.64)	10	0.72 (1.38)	0.77 (1.87)	0.75 (1.82)
MP AV	10	0.86 (1.41)	0.71 (1.32)	0.25 (0.60)	10	0.76 (1.28)	0.63 (1.51)	0.32 (0.98)
MP RD	10	0.78 (1.34)	0.66 (1.26)	0.27 (0.65)	10	0.77 (1.52)	0.70 (1.87)	0.57 (1.20)
MI TRI	10	0.88 (1.35)	0.73 (1.31)	0.19 (0.69)	10	0.85 (1.51)	0.71 (1.39)	0.31 (0.95)
MI PV	10	0.89 (1.24)	0.74 (1.13)	0.11 (0.32)	10	0.89 (1.24)	0.74 (1.09)	0.13 (0.37)
method	PET -> noisy MR				noisy MR -> PET			
MP QU	10	0.86 (1.50)	0.71 (1.39)	0.40 (1.04)	10	0.80 (2.18)	0.73 (2.06)	0.54 (1.32)
MP AV	10	0.78 (1.47)	0.66 (1.42)	0.35 (0.83)	10	0.83 (1.84)	0.71 (1.80)	0.43 (1.15)
MP RD	10	0.85 (1.76)	0.71 (1.34)	0.37 (0.91)	10	0.60 (1.35)	0.58 (1.51)	0.50 (1.23)
MI TRI	10	0.88 (1.24)	0.73 (1.20)	0.23 (0.67)	10	0.88 (1.98)	0.73 (1.56)	0.45 (1.03)
MI PV	10	0.90 (1.20)	0.75 (1.12)	0.18 (0.46)	10	0.60 (1.34)	0.50 (0.87)	0.20 (0.57)
method	PET -> noisy MR with bias field				noisy MR with bias field -> PET			
MP QU	10	0.72 (1.55)	0.61 (1.41)	0.43 (1.02)	10	0.70 (1.82)	0.61 (2.16)	0.49 (1.24)
MP AV	10	0.72 (1.51)	0.61 (1.44)	0.38 (1.00)	10	0.63 (1.22)	0.55 (1.37)	0.38 (1.15)
MP RD	10	0.72 (1.29)	0.61 (1.16)	0.41 (0.95)	10	0.57 (1.26)	0.52 (1.40)	0.52 (1.80)
MI TRI	10	0.83 (1.21)	0.70 (1.28)	0.40 (0.77)	10	0.88 (1.65)	0.75 (1.88)	0.61 (1.78)
MI PV	10	0.84 (1.13)	0.70 (1.27)	0.44 (0.74)	10	0.59 (0.90)	0.49 (1.02)	0.41 (0.76)

anatomical reference points in the MR and PET images. The registrations were scored using the following scale: very good, good and bad. The outcome of the analysis can be found in Table II. All data sets could be registered good to very

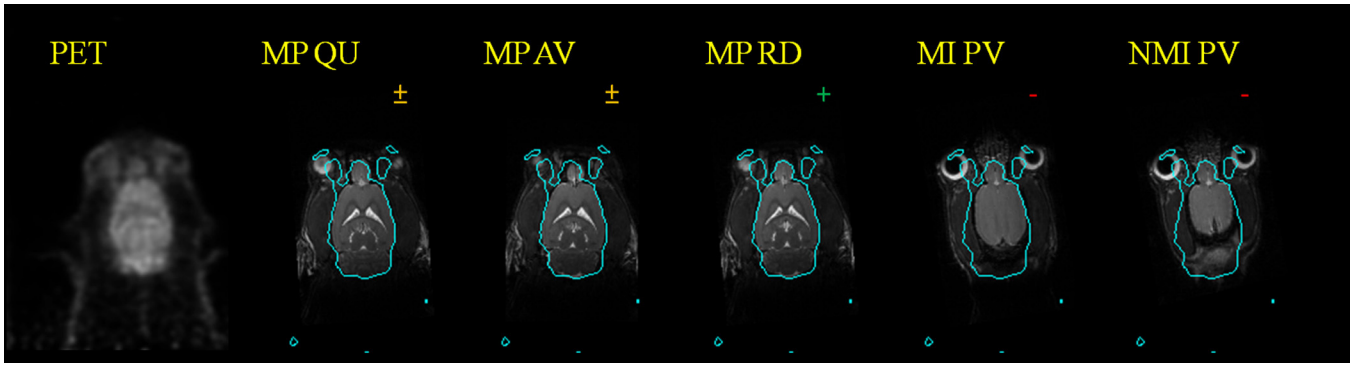

Fig. 5. Example registered images of one rat. Coronal slices through the PET image, and through the corresponding slices in the MR image, registered using the quadratic, absolute value and relative difference MP-based criterion, and using mutual information and normalized mutual information with partial volume interpolation.

good using the MP registration algorithms, whereas only 70% were aligned good to very good using MI or NMI. Even more convincing is the fact that up to 80% were classified as very good using an MP criterion (even 90% if different similarity measures can be used for different data sets), compared to only 10% using MI or NMI. The registration accuracy of NMI was for all rats very similar to that of MI. To illustrate the different registration accuracy levels, the registered images of a rat with variable registration performance for the different methods are shown in Fig. 5.

D. Mouse Brain Data

As can been seen from the example registered images shown in Fig. 6, all MP methods yielded a good microMR to microPET registration, whereas the registrations obtained with MI and NMI were less accurate. Except for the manual initialization, no additional processing steps (e.g., masking or bias field correction) were required.

VI. Discussion

Registration of MR to PET images, as well as MR to MR images, using mutual information is challenging in the presence of strong MR intensity inhomogeneity, such as typically induced by the use of surface coils in small animal MR imaging. Usually, brain masking and bias field correction steps are required to enable a good alignment [14]. The studies presented in this paper show that Markov prior-based registration algorithms are capable of aligning an FDG PET human brain image to a T1-weighted MR image, as well as registering an FDG microPET brain image to an MR image obtained using a 3D turboRARE sequence, even in the presence of noise or bias field. If the images are initially brought close enough to each other (max. rotation: 5°, max. translation: 10 mm), usually a mean registration accuracy below 0.9 mm and a maximum registration accuracy of about 1.5 mm in all directions can be achieved for the human brain images. This accuracy was found to be comparable to that of MI, especially if the MR suffers from a bias field. Therefore, case studies with real MR images with a severe bias field artifact, causing registration problems for MI, were selected for further evaluation of the proposed methods. The local character of the presented criteria has been proven to be an advantage for these real life cases.

It is to be expected that these MP algorithms can also be applied to register images obtained from different imaging modalities (e.g. SPECT, CT, ...), using various tracers or contrast agents, and using different acquisition protocols (e.g. T2-weighted MRI), but it requires extensive evaluation studies to test the stability and accuracy for each application. Furthermore, they can be extended to perform non-rigid registration.

VII. Conclusion

A new set of algorithms was presented for accurate multimodality image registration. They are based on an anatomical Markov prior and are robust against noise and bias fields in MR images. The achieved accuracy is close to that of MI for aligning FDG PET and T1-weighted MR images of a human brain. In the presence of a strong bias field (e.g., in microMR images due to the use of surface coils), the proposed registration algorithms clearly outperform MI and NMI.

Acknowledgment

The authors would like to thank Cindy Casteels for visually scoring the registration accuracy of small animal brain data sets.

References

[1] F. Maes, A. Collignon, D. Vandermeulen, G. Marchal, P. Suetens. "Multimodality image registration by maximization of mutual information", IEEE Trans. Med. Imaging, vol. 16, no. 2, pp. 187-198, 1997.

[2] C. Studholme, D. L. G. Hill, D. J. Hawkes. "An overlap invariant entropy measure of 3D medical image alignment", Pattern Recognition, vol. 32, no. 1, pp. 7186, 1999.

[3] S. Somayajula, E. Asma, R. M. Leahy. "PET image reconstruction using anatomical information through mutual information based priors", IEEE Nucl. Sci. Symp. Conf. Record, 2005, pp. 2722-2726.

[4] J. Nuyts. "The use of mutual information and joint entropy for anatomical priors in emission tomography", IEEE Nucl. Sci. Symp. Conf. Record, 2007, pp. 4149-4154.

[5] J. E. Bowsher, H. Yuan, L. W. Hedlund, T. G. Turkington, G. Akabani, A. Badea, W. C. Kurylo, C. T. Wheeler, G. P. Cofer, M. W. Dewhirst, G. A. Johnson. "Using MRI information to estimate F18-FDG distributions in rat flank tumors", IEEE Nucl. Sci. Symp. Conf. Record, 2004, pp. 2488-2492.

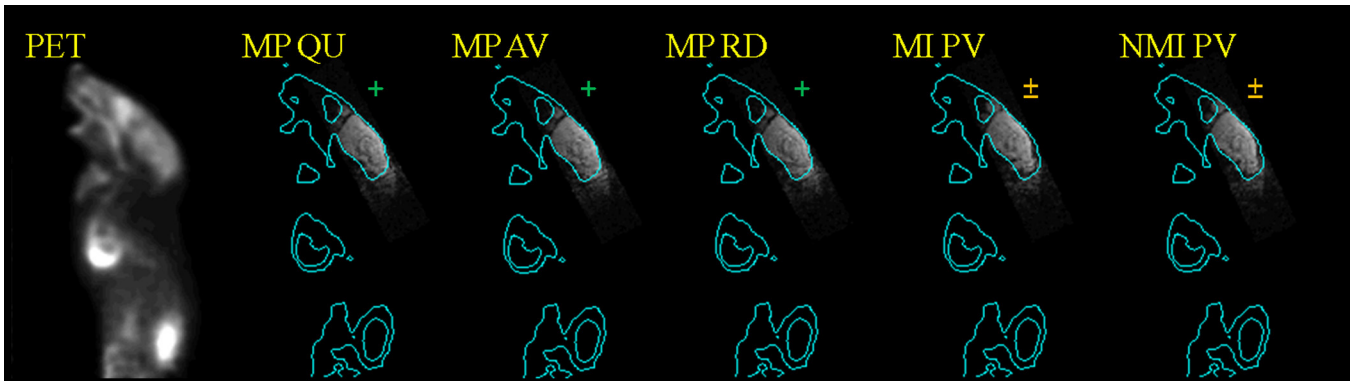

Fig. 6. Example registered images of the mouse. Sagittal slices through the PET image, and through the corresponding slices in the MR image, registered using the quadratic, absolute value and relative difference MP-based criterion, and using mutual information and normalized mutual information with partial volume interpolation.

[6] A. Bousse, S. Pedemonte, D. Kazantsev, S. Ourselin, S. Arridge, B. F. Hutton. "Weighted MRI-based Bowsher priors for SPECT brain image reconstruction", IEEE Nucl. Sci. Symp. Conf. Record, 2010, pp.3519-3522.

[7] D. Kazantsev, A. Bousse, S. Pedemonte, S. R. Arridge, B. F. Hutton, S. Ourselin. "Edge preserving Bowsher prior with nonlocal weighting for 3D spect reconstruction", IEEE International Symposium on Biomedical Imaging: From Nano to Macro, 2011, pp. 1158-1161.

[8] K. Vunckx, A. Atre, K. Baete, A. Reilhac, C. M. Deroose, K. Van Laere, J. Nuyts. "Evaluation of three MRI-based anatomical priors for quantitative PET brain imaging", IEEE TRANSACTIONS ON MEDICAL IMAGING, in press.

[9] C. Bouman, K. Sauer. "A generalized Gaussian image model for edge-preserving MAP estimation", IEEE Trans. Image Process., vol. 2, no. 3, pp. 296-310, 1993.

[10] J. Nuyts, D. Bequé, P. Dupont, L. Mortelmans. "A concave prior penalizing relative differences for maximum-a-posteriori reconstruction in emission tomography", IEEE Trans. Nucl. Sci., vol. 49, no. 1, pp. 56-60, 2002.

[11] website: "http://www.bic.mni.mcgill.ca/brainweb/"

[12] D. L. Collins, A. P. Zijdenbos, V. Kollokian, J. G. Sled, N. J. Kabani, C. J. Holmes, A. C. Evans. "Design and construction of a realistic digital brain phantom", IEEE Trans. Med. Imaging, vol. 17, no. 3, pp. 463-468, 1998.

[13] C. Casteels, C. Vandeputte, J. R. Rangarajan, T. Dresselaers, O. Riess, G. Bormans, F. Maes, U. Himmelreich, H. Nguyen, K. Van Laere. "Metabolic and Type 1 cannabinoid receptor imaging of a transgenic rat model in the early phase of Huntington disease", Experimental Neurology, vol. 229, no. 2, pp. 440-449, 2011.

[14] J. R. Rangarajan, D. Loeckx, G. Vande Velde, T. Dresselaers, U. Himmelreich, F. Maes, P. Suetens. "Impact of RF inhomogeneity correction on image registration of micro MRI rodent brain images", 8th IEEE international symposium on biomedical imaging - ISBI 2011, pp. 570-573, March 30-April 2, 2011, Chicago, Illinois, USA.